

Mitochondrial Mode of Action of a Thymidine-Based Cisplatin Analogue Breaks Resistance in Cancer Cells

Liliane A. Onambele,^[a] Daniel Koth,^[b] Justyna A. Czaplewska,^[b] Ulrich S. Schubert,^[b] Helmar Görls,^[c] Shigenobu Yano,^[d] Makoto Obata,^[e] Michael Gottschaldt,^{*[b]} and Aram Prokop^{*[a]}

Abstract: Cisplatin analogue complexes with platinum(II) and palladium(II) starting from 3',5'-diamino-3',5'-dideoxy-thymidines were synthesized, both with the *D-erythro*- and *D-threo* configurations. Complexes of the general formula [MCl₂L] were obtained and characterized. NMR spectroscopic measurements and single crystal X-ray structure analysis showed that the metal centers are coordinated to the ligands by the amino groups in 3'- and 5'-positions and not through the thymine moiety. All ligands and complexes showed no significant in vitro

activities except thymi-platin (*cis*-dichloro(3',5'-diamino-3',5'-dideoxy-*D-threo*-thymidine)platinum(II)). Detailed in vitro studies on the apoptosis pathway in lymphoma (BJAB), leukemia (NALM-6), and melanoma cells (Mel-HO) as well as on transfected or resistant cell lines were carried out. Thymi-platin significantly induced an apoptotic response, which was found to

be associated with the loss of mitochondrial membrane potential and with caspase activation. The activity was shown to be independent of Fas-associated protein with death domain (FADD), but dependent on Bcl-2 expression. As a consequence, for thymi-platin a mitochondrial mode of action could be assigned. Moreover, the compound showed activity in cells resistant to common drugs, such as daunorubicin and vincristin, and showed synergistic effects with doxorubicin, vincristin, cytarabine, and daunorubicin.

Keywords: antitumor agents · apoptosis · drug resistance · nucleosides · platinum

Introduction

Since the discovery of cisplatin as a potent antitumor agent,^[1] platinum-based anticancer drugs have been constantly advanced and modified.^[2] In current oncology, three approved platinum drugs play a major role: cisplatin, carboplatin, and oxaliplatin. Additionally, combinations of picoplatin or satraplatin with, for example, paclitaxel, against certain types of cancer, are under investigation for approval.^[3] The major mechanism of action of these platinum-based drugs is the formation of DNA adducts by binding to the N7 sites of purine bases of the double strand to form interstrand cross-links.^[4] This results in several analogous pathways for resistance to these compounds, such as reduced intracellular drug accumulation, inactivation by thiol containing molecules, or enhanced DNA repair, and has led to an extensive search for compounds with different principles of operation or enhanced selectivity.^[5,6] Efforts include the use of polymeric vehicles for target-selective delivery of platinum-based anticancer agents,^[7] the development of active complexes of various metal ions as well as their conjugation with biomolecules.^[8]

[a] L. A. Onambele, Dr. A. Prokop
Children's Hospital of the City of Cologne
Amsterdamerstr. 59, 507335 Cologne (Germany)
Fax: (+49) 3641948202
E-mail: prokopa@klinik-koeln.de

[b] Dr. D. Koth, Dr. J. A. Czaplewska, Prof. U. S. Schubert,
Dr. M. Gottschaldt
Laboratory for Organic and Macromolecular Chemistry (IOMC)
Friedrich-Schiller-University Jena, Humboldtstr. 10
07743 Jena (Germany)
Fax: (+49) 3641948202
E-mail: michael.gottschaldt@uni-jena.de

[c] Dr. H. Görls
Institute for Inorganic and Analytical Chemistry
Friedrich-Schiller-University Jena, Lessingstr. 8
07743 Jena (Germany)

[d] Prof. S. Yano
Nara Institute of Science and Technology (NAIST)
8916-5, Takayama-cho, Ikoma, Nara 630-0192 (Japan)

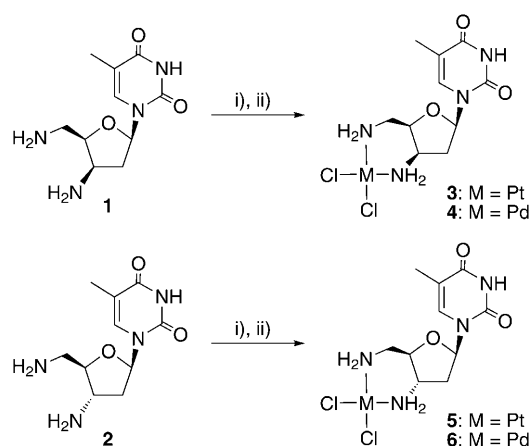
[e] Dr. M. Obata
Interdisciplinary Graduate School of Medicine and Engineering
University of Yamanashi, Takeda 4-4-37, Kofu 400-8510 (Japan)

Supporting information for this article is available on the WWW under <http://dx.doi.org/10.1002/chem.201000785>.

In contrast to the well-explored carbohydrate-based metal complexes and in particular to their platinum compounds,^[9–11] the corresponding nucleoside analogues seem to be virtually unexplored. Only a very few isolated platinum complexes bearing nucleoside ligands are known, although studies on the uptake of nucleosides and their derivatives by different membrane-bound transport proteins have shown that their uptake is less hindered than for monosaccharide-based molecules.^[12] Iron containing nucleoside analogues show promising antitumor activities.^[13,14] Compounds based on N-aminated nucleosides have been studied both in vivo and in vitro. Their cytotoxic effect against L1210 cells in vitro was found to be ten-times lower than that of cisplatin, and in vivo they did not exhibit any antitumor activity.^[15] A cisplatin analogue with an ethylenediamine ligand that is linked via a propyl group to thymidine was also described.^[16] The number of studied compounds in which the sugar part of the nucleoside is used for the complexation of platinum(II) is much smaller. All compounds studied so far have possessed the *D-erythro* configuration. Among them, a dose dependent increase in survival time in mice bearing the L1210 tumor was only observed for the dichlorobis(3'-amino-3'-deoxy-*D-erythro*-thymidine)-platinum(II) complex.^[17] Although the mode of action could not be assigned clearly, it has been assumed that the kind of nucleobase and sugar unit has a strong influence on the antiproliferative activity of the corresponding complexes. Inspired by the strong dependency of biological activity on the configuration of diaminosaccharides and -nucleosides attached to metal ions,^[11,17] the respective *D-threo* configured derivative of thymidine with a pseudo-axial arrangement of the amino group in the 3'-position was used to coordinate platinum(II) in the present study. For comparison, the analogue *D-erythro* derivative^[17] as well as the palladium complexes were also synthesized and tested for their antitumor activity in vitro.

Results and Discussion

Synthesis and structural characterization of the complexes: The two 3',5'-diamino-3',5'-dideoxy-thymidines (**1** and **2**) were previously obtained as intermediates for the synthesis of metal complexes based on their condensation products with salicyliden aldehydes.^[18,19] The synthesis pathway applied is much more efficient than the introduction of two amino groups into uridine in the 2',3'-position or into *D*-ribose or 2-deoxy-*D*-ribose,^[20,21] because the thymine residue acts as a protecting group of the 3'-position during the synthesis (see Scheme S1 in the Supporting Information). For the preparation of the platinum (**3** and **5**) and palladium complexes (**4** and **6**) an aqueous solution of potassium tetrachloroplatinate or potassium tetrachloropalladate, respectively, was added dropwise into a boiling solution of the amine (**1** or **2**) in water (Scheme 1). After a short time, the formed complexes precipitated. Uncharged stable complexes with Pt^{II} and Pd^{II} of the general formula [MCl₂L] were formed, as shown by mass spectrometry and NMR



Scheme 1. Schematic representation of the synthesis of platinum(II) and palladium(II) complexes of 3',5'-diamino-3',5'-dideoxy-thymidine with either the *D-threo* (**1**) or *D-erythro* configuration (**2**). i) K₂[PtCl₄], H₂O, reflux, > 90%; ii) K₂[PdCl₄], H₂O, reflux, > 90%.

spectroscopic measurements. Crystallization of complex **4** by using ethanol and water resulted in crystals suitable for single crystal X-ray structure analysis (Figure 1). The asym-

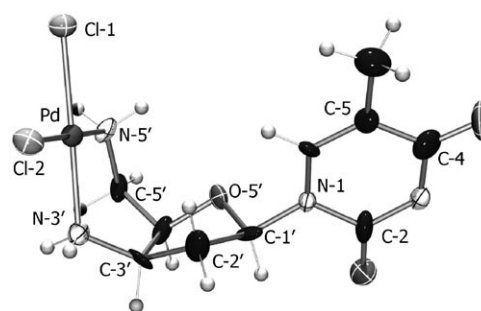


Figure 1. X-ray single crystal structure of a molecule in the crystal of the palladium complex **4** with numbering according to NMR spectroscopy. Atomic displacement parameters are drawn at the 50% probability level.

metric unit of the crystal contains two symmetrically independent molecules of **4** and two water molecules that are neither involved in the complexation nor bound to the ligands. There is only a very small difference between the two complex molecules within the asymmetric unit. As suspected, the palladium(II) ion has a square planar coordination geometry (Table 1). One side of the complex is sterically shielded by the nucleobase. The nucleobase, which usually serves to coordinate metal ions, is not involved in the coordination of the metal ion. As expected from the crystal

Table 1. Selected bond lengths (Å) and angles (°) of complex **4**.^[a]

Pd–N-5'	2.022(11)	N-5'–Pd–N-3'	90.8(4)
Pd–N-3'	2.038(12)	N-5'–Pd–Cl-1	87.4(3)
Pd–Cl-1	2.301(4)	N-3'–Pd–Cl-2	89.4(4)
Pd–Cl-2	2.315(4)	Cl-1–Pd–Cl-2	92.33(13)

[a] The dihedral angle at the palladium center between the planes defined by Pd–N-5'–Cl-1 and Pd–N-3'–Cl-2 is 0.87°.

structure of **4**, also the NMR signals of the nucleobases of the other complexes show no significant shifts compared to those of the free ligands. These results prove that the thymine is not involved in the coordination of the metals since coordination to platinum or palladium would result in a high-field adjustment.

To investigate the stability of the platinum(II) complex **3** compared with cisplatin, AgNO₃ was added to an aqueous solution of compound **3** and the precipitate was filtered off. Mass spectrometric measurement of the solution showed the complete disappearance of **3** (*m/z* 533) and the formation of a new product with *m/z* 511 in which one chloride is exchanged against a water molecule, analogous to cisplatin (Figure S1 in the Supporting Information). Treatment of **3** with 5'-GMP in PBS buffer resulted in the formation of a mono-adduct of the general formula [PtCl(5'-GMP)L]⁺, which was detected by ESI-MS measurements (Figure S2 in the Supporting Information). This is similar to the treatment of cisplatin with nucleotides, and shows that platinum complex **3** is able to exchange chloride ions and bind to biological targets, and therefore, should exhibit biological activity.

In vitro activities of compounds 1–6: To investigate the biological activity of the synthesized compounds, their antiproliferative and apoptotic properties were screened by using lymphoma cells (BJAB). The pure ligands (**1** and **2**) and the palladium(II) derived compounds (**4** and **6**) had no significant effects (Figure S3 in the Supporting Information). The Pt^{II} complex with the *D-erythro* configuration (**5**) exhibited comparably small antiproliferative activity (50% after 72 h incubation at 80 μM). Only thymiplitin (**3**; *cis*-dichloro(3',5'-diamino-3',5'-dideoxy-*D-threo*-thymidine)-platinum(II)) possessed significant activity (80% growth inhibition after 96 h incubation at 40 μM and 50% apoptosis after 96 h at 60 μM; Figures 2A and 3A). Therefore, only the antitumor activity of the nucleoside analogue thymiplitin (**3**) was investigated in more detail with lymphoma (BJAB), leukemia (NALM-6), and melanoma cells (Mel-HO) *in vitro*.

Leukemia is the most common malignant disease in childhood. Approximately one third of cancer patients have a type of leukemia, most commonly acute lymphoblastic leukemia (ALL). Significant research into the causes, diagnosis, treatment, and prognosis of leukemia is being carried out. Despite a relatively good prognosis, approximately one quarter of the patients suffer from relapse and, consequently, a worse outlook. Furthermore, resistance is a serious drawback with many existing antileukemia drugs. It has been suggested that most chemotherapeutics exert their effects by triggering apoptotic cell death. Accordingly, drug-induced apoptosis in tumor and leukemia cells predicts the response of the therapy. BJAB and NALM-6 cells were chosen because cisplatin shows low activity against them and cannot be applied in the therapy of leukemia and Burkitt lymphoma leukemia.

Determination of apoptosis induced by thymiplitin: Apoptosis represents an important factor in maintaining homeo-

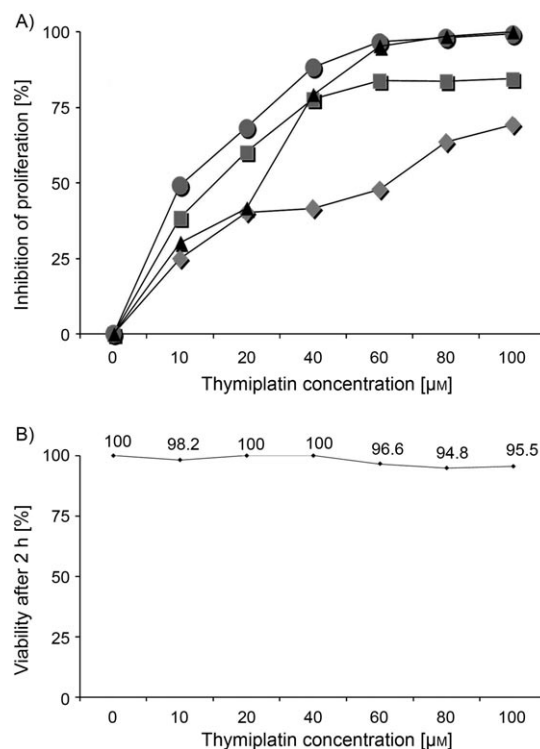


Figure 2. Inhibition of proliferation and cell viability. A) BJAB cells were treated with different concentrations of thymiplitin (**3**). After incubation for different lengths of time (◆=24, ■=48, ●=72, ▲=96 h), proliferation was measured by using the Casy count system. Values are given as percentages of inhibition of cell proliferation (error bars are omitted for clarity). B) BJAB cells were treated with different concentrations of **3** for 2 h. Viability was determined by the LDH release assay. Values are given as percentages of the control.

stasis and elimination of damaged cells.^[22] Many anticancer drugs act by causing the death of tumor cells through the induction of apoptosis.^[23] Apoptosis is a mode of cell death that appears under normal physiological condition or pharmacological stimuli. The cell is an active participant in its own destruction. Apoptosis plays an important role in the regulation of cell number or in the elimination of damaged cells. Cells undergoing apoptosis show segmentation of the cytoplasm and nucleus into apoptotic bodies. *In vivo*, they are rapidly recognized and phagocytized, so that no inflammatory response is involved in apoptosis. In contrast, necrotic cell death is often associated with extensive tissue damage resulting in a strong inflammatory response, *in vivo*.

Incubation of BJAB cells with 10 to 100 μM of **3** led to a statistically significant decrease in cell viability after 48 h (data not shown). There was up to 100% time- and concentration-dependent inhibition of cell proliferation after 72 h incubation (Figure 2A). A decrease in cell counts might be due to cell necrosis or apoptosis.^[24] To show that the decrease in proliferation was due to apoptosis and not to necrosis, lactate dehydrogenase, which is an enzyme that is released by plasma membrane lysis and is characteristic of cell necrosis while apoptotic cells maintain their membrane integrity,^[25] was shown to be absent in culture supernatants of BJAB cells incubated for 2 h with 10–100 μM of **3** (Fig-

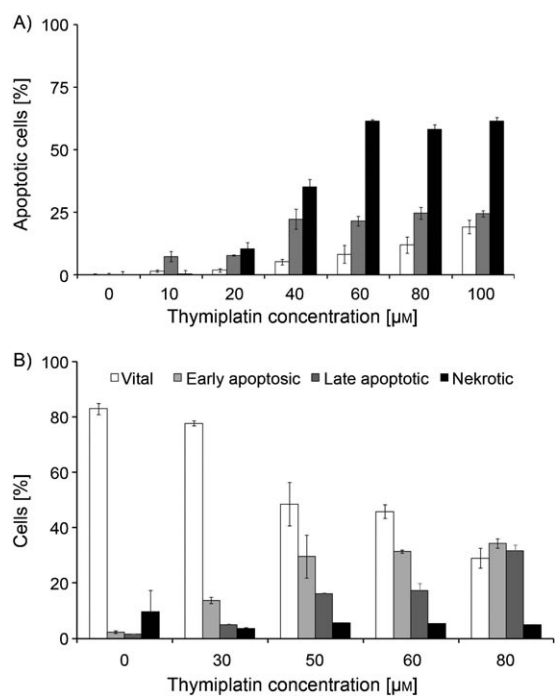


Figure 3. Apoptosis induction: A) BJAB cells were treated with different concentrations of **3**. After incubation for different lengths of time ($\square = 48$, $\blacksquare = 72$, $\blacksquare = 96$ h), DNA fragmentation was measured by flow cytometric analysis of cellular DNA content. Values are given as percentages of cells with hypodiploid DNA \pm S.D. ($n=3$). B) BJAB cells were incubated with different concentrations of **3** for 48 h. Early and late apoptosis was measured after annexin V/PI staining by using flow cytometry. Values are given as percentages of annexin V+/PI- cells \pm S.D. ($n=3$).

ure 2B). Additionally, effects of **3** were studied with respect to DNA fragmentation, a hallmark of apoptotic cells, which occurs at the end of apoptosis.^[25] This was shown to increase in a time- and dose-dependent manner in the range of concentrations of **3** tested. Thus, **3** significantly induces DNA fragmentation in up to 60% of cells with a half maximal concentration (AC_{50}) of 50 μ M (Figure 3A). Remarkably, the most significant effects occurred after 96 h of incubation, which is a comparably long time for platinum-based agents. Distinct early- and late-phase apoptotic BJAB cells were found after treatment with **3**, as shown by annexin V/propidium iodide (PI) staining (Figure 3B). A significant induction in necrosis was not found. Taken together, these data indicate that **3** specifically induces apoptosis in the BJAB lymphoma cell line (in contrast to the very low activity of cisplatin with 14% apoptotic BJAB cells after 72 h incubation at 100 μ M; see Figure S4 in the Supporting Information).

Investigation of the induced apoptotic pathway: The process of apoptosis is controlled by a diverse range of cell signals, which can originate either extracellularly (extrinsic pathway, type I apoptosis) or intracellularly (intrinsic pathway, type II apoptosis). The type I apoptosis cascade is triggered by the membrane-anchored Fas-receptor (CD95/Fas) and involves the proapoptotic protein for the extrinsic pathway FADD

(Fas-associated protein with death domain). The intrinsic or mitochondrial pathway of apoptosis (type II) is associated with changes in the permeability of the outer mitochondrial membrane and the collapse of the membrane potential.^[26] Caspase-9 is the initiator of this pathway and caspase-3 is a key executioner of apoptosis.^[27,28] Mitochondrial outer membrane permeabilization is governed by anti- and pro-apoptotic members of the Bcl-2 protein family.^[29]

To investigate the involvement of CD95/Fas (type I apoptosis), BJAB cells over-expressing a dominant-negative FADD (FADD-dn) mutation were used alongside control cells. Treatment of both mutant and control cells with different concentrations of **3** indicates that with up to 50 μ M the apoptosis produced is independent of CD95/Fas, as shown by DNA fragmentation analysis (Figure 4). However, at concentrations above 50 μ M, thymiaplantin-induced apoptosis is partly dependent on FADD-dn expression; this implies the partial involvement of the extrinsic apoptosis pathway with higher concentrations.

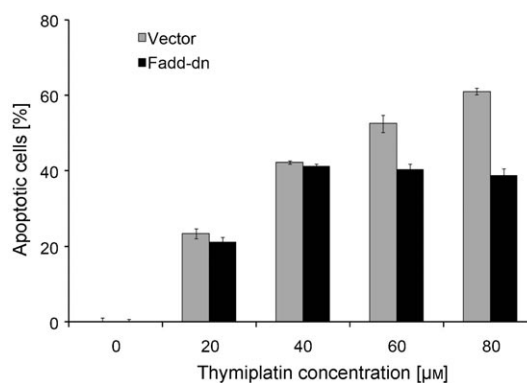


Figure 4. Dependence and independence of the apoptosis induced by **3** on the over-expression of FADD-dn in BJAB cells. Vector- (gray) and FADD-dn-transfected (black) BJAB cells were incubated with different concentrations of the agent for 72 h. Subsequently, DNA fragmentation was measured by flow cytometric analysis of cellular DNA content. Values are given as percentages of cells with hypodiploid DNA \pm S.D. ($n=3$).

To determine whether apoptosis induced by **3** is mediated through the mitochondrial pathway (type II apoptosis), BJAB cells treated with different concentrations of **3** were stained with JC-1 and mitochondrial activation was evaluated. Flow cytometric analysis of mitochondrial permeability transition revealed a concentration-dependent disruption of membrane potential in up to 28% of the cell population (Figure 5). Furthermore, we could show by Western blot analysis of BJAB cells treated with **3** that caspases-3 and -9 are processed, respectively, to the active p17 subunit and the 37 kDa product (Figure 6). To determine the role of Bcl-2 (an antiapoptotic protein in the intrinsic pathway) in apoptosis induced by **3**, Mel-HO/bcl-2 melanoma cell lines transfected to over-express Bcl-2 were incubated with different concentrations of **3**. The results show that apoptosis induced by the compound is dependent on Bcl-2 levels at 72 and 96 h (data shown for 72 h of incubation in Figure 7).

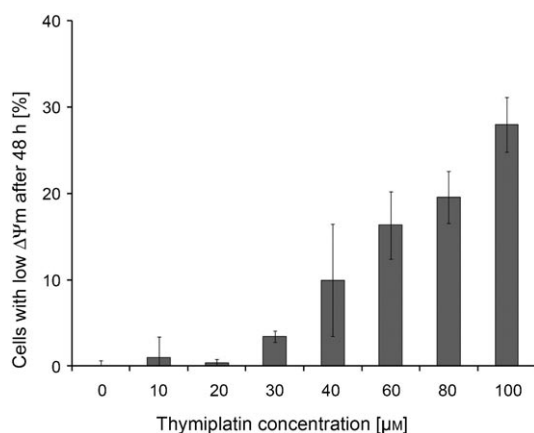


Figure 5. Inhibition of mitochondrial permeability transition. BJAB cells were incubated with different concentrations of **3** for 48 h. Subsequently, mitochondrial permeability transition was measured by flow cytometry on a single cell level. Values of mitochondrial permeability transition are given as percentages of cells with low mitochondrial membrane potential \pm S.D. ($n=3$).

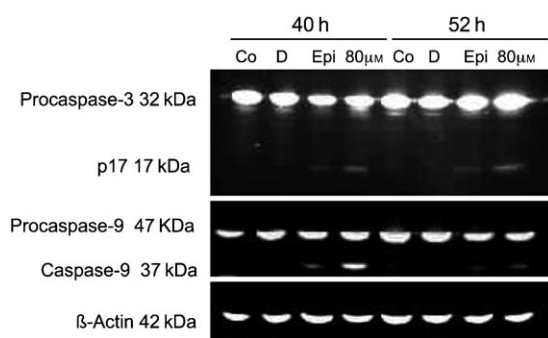


Figure 6. Compound **3** induces caspase-9 and caspase-3 activation. BJAB cells were incubated either with **3** (80 μM) or epirubicin (5 μM) as the positive control. After 40 and 52 h of incubation, the cells were collected and lysed. Cytosolic protein (40 μg) was separated by sodium SDS-PAGE and subjected to Western blot analysis. Immunoblots probed with anti-caspase-3, anti-caspase-9, and anti-β-actin antibodies are shown. The position of the 17 kDa active subunit of caspase-3 and the 37 kDa active subunit of caspase-9 are indicated. Equal loading and blotting was verified by detection of β-actin.

We could demonstrate a dose- and time-dependent inhibition of the proliferation (Figure 2B) of cancer cells after treatment with **3**. The processing of caspase-3 (Figure 6) could be visualized and the rate of DNA fragmentation determined (Figure 3A). These results suggest that **3** induces apoptosis in tumor cells. The activation of caspase-3 correlated with the activation of caspase-9 (Figure 6). Consistent with an early disruption of the mitochondrial membrane potential (Figure 5), we have demonstrated that the intrinsic pathway probably mediates thymiplitin-induced apoptosis. The dependence of thymiplitin-induced apoptosis on Bcl-2 over-expression and its independence of FADD expression up to a concentration of 40 μM (Figure 4) further implicates the intrinsic pathway in thymiplitin-induced apoptosis. At higher concentrations (>40 μM), **3** is able to induce apoptosis through the extrinsic pathway (Figure 4), which is possi-

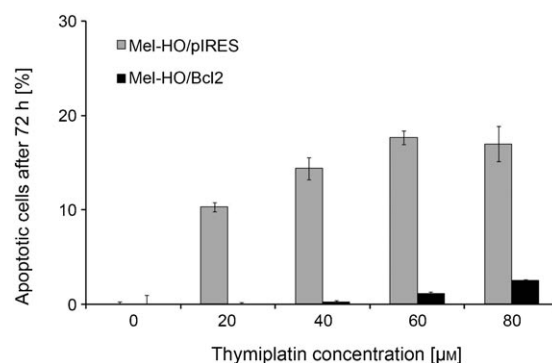


Figure 7. Dependence of thymiplitin-induced apoptosis on the over-expression of Bcl-2 in Mel-HO cells. Vector-*bcl-2*-transfected Mel-HO cells were treated with different concentrations of **3** for 72 h. DNA fragmentation was measured by flow cytometric analysis of cellular DNA content. Values are given as percentages of cells with hypodiploid DNA \pm S.D. ($n=3$).

ble in clone cells that over-express the anti-apoptotic protein Bcl-2 by 30-fold (Figure 7).

Activity of thymiplitin against resistant cells and synergistic effects: Drug resistance is a serious drawback for many existing anticancer drugs.^[30] One way to overcome the problem of drug resistance is to develop new drugs.^[31] However, an attractive alternative is the production of drugs that are synergistic to existing ones.^[31] In order to investigate whether thymiplitin (**3**) could be effective with vincristin and daunorubicin resistance, different concentrations of **3** were used to treat resistant cell lines (NALM-6/VCR and Nalm-6/DAUNO) for 72 h. Interestingly, thymiplitin was effective in inducing apoptosis in these cell lines as shown by DNA fragmentation analysis (Figure 8). Compared to cisplatin (see Figure S4 in the Supporting Information) thymiplitin possesses a higher activity against NALM-6 as well as their resistant variants. Subsequently, we investigated whether **3** could have any synergistic effects with other common drugs. Therefore, BJAB cells were incubated with low concentrations of **3** in combination with low concentrations of cytarabine, vincristin, daunorubicin, and doxorubicin. Thymiplitin was synergistic with all drugs tested as shown by DNA fragmentation analysis at 72 and 96 h (Figure 9).

Conclusion

In conclusion, we have synthesized new platinum(II) and palladium(II) thymidin-based complexes of the general formula $[MCl_2L]$. The coordination of the metal ions is realized by the amino groups introduced in the 3'- and 5'-positions for both classes with the *D-erythro* and *D-threo* configurations, whereas the nucleobase is not involved. The ligands as well as the palladium(II) complexes were found to possess no significant cytotoxicity. In contrast, the absolute configuration at the 3'-position of the platinum(II) complexes has a major impact on their biological activity. Only for the platinum complex with the *D-threo* configuration (**3**, thymiplitin)

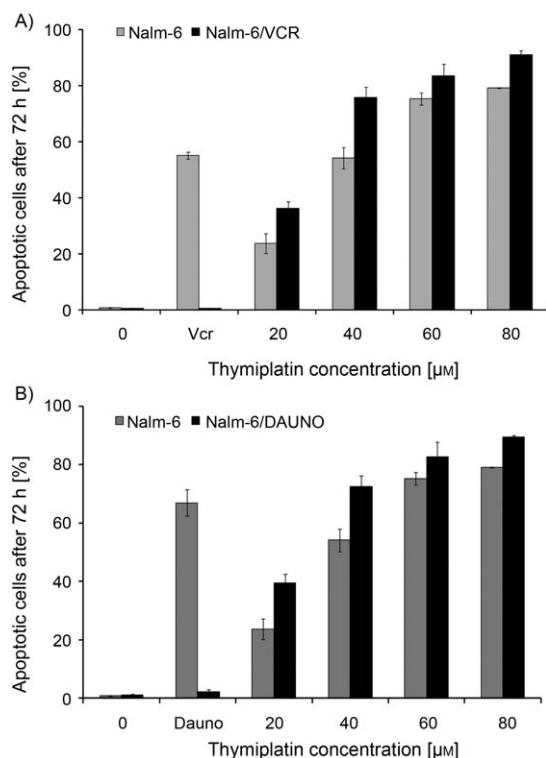


Figure 8. Overcoming: A) vincristin, and B) daunorubicin resistance in NALM-6 cells. Wild-type and resistant cells were treated with different concentrations of thymioplatin for 72 h. Then, DNA fragmentation was measured by flow cytometry of cellular DNA content. Values are given as percentages of cells with hypodiploid DNA \pm S.D. ($n=3$).

notable antiproliferative and cytotoxic activity could be observed.

Thymioplatin inhibits proliferation and specifically induces apoptosis in lymphoma cell lines. The induced apoptosis is mediated by caspase-9 and -3 processing, which is characterized by a loss of mitochondria membrane potential and is dependent on Bcl-2. Further, it is independent of CD95/Fas signaling. Therefore, a mitochondrial mode of action can be assigned to thymioplatin. Moreover, it is active on vincristin and daunorubicin resistant leukemia cells. Additionally, synergistic effects with cytarabine, vincristin, daunorubicin, and doxorubicin could be shown with lymphoma cells.

Experimental Section

General procedure for the synthesis of the metal complexes: $K_2[PtCl_4]$ or $K_2[PdCl_4]$ (0.624 mmol) dissolved in water (5 mL) were added dropwise to a solution of the respective 3',5'-diamino-3',5'-dideoxythymidine (**1** or **2**; 150 mg, 0.625 mmol) in boiling water (20 mL). Within a few minutes a precipitate was formed. To complete the complex formation, the reaction mixture was stirred for 5 h and stored, overnight, in a refrigerator. The precipitate formed was filtered off. To increase the yield of the target compound, the filtrate was concentrated and the precipitates formed were combined and washed successively with cold water, cold ethanol, and diethyl ether, and finally dried under vacuum.

cis-Dichloro(3',5'-diamino-3',5'-dideoxy-D-threo-thymidine)platinum(II) (3): With ligand **1** and $K_2[PtCl_4]$ (259.15 mg, 0.624 mmol); yield 301 mg (95%); 1H NMR (400 MHz, $[D_6]DMSO$): $\delta = 11.38$ (s, 1H; NH), 7.90 (s,

1H; H-6), 6.21–5.89 (m, 5H; H-1', NH₂), 4.28 (m, 1H; H-4'), 3.78 (m, 1H; H-3'), 3.10–2.83 (m, 2H; H-5', H-5''), 2.70–2.64 and 2.59–2.53 (2m, 2H; H-2', H-2''), 1.83 ppm (s, 3H; $-CH_3$); ^{13}C NMR (100 MHz, $[D_6]DMSO$): $\delta = 163.7$ (C-4), 150.4 (C-2), 136.2 (C-6), 110.1 (C-5), 82.24 (C-4'), 75.3 (C-1'), 52.5 (C-3'), 40.9 (C-5'), 38.0 (C-2'), 12.2 ppm ($-CH_3$); IR (ATR): $\tilde{\nu}_{max} = 3489, 3196, 3109, 2826, 1673, 1469, 1369, 1267, 1109, 1047, 958, 761, 666$ cm^{-1} ; MS (ESI): $m/z = 528.1$ $[M+Na]^+$, 543.0 $[M+K]^+$; elemental analysis calcd (%) for $C_{10}H_{16}Cl_2N_4O_3Pt$: C 23.73, H 3.19, N 11.07; found: C 23.13, H 3.38, N 10.48.

cis-Dichloro(3',5'-diamino-3',5'-dideoxy-D-threo-thymidine)palladium(II) (4): With ligand **1** and $K_2[PdCl_4]$ (203.8 mg, 0.624 mmol); yield 246 mg (94%); 1H NMR (250 MHz, $[D_6]DMSO$): $\delta = 10.08$ (s, 1H; NH), 7.51 (s, 1H; H-6), 6.00 (m, 1H; H-1'), 5.0–4.3 (m, 4H; NH₂), 3.71 (m, 1H; H-3'), 3.42–3.53 (m, 3H; H-4', H-5', H-5''), 2.24–2.09 (m, 2H; H-2', H-2''), 1.80 ppm (s, 3H; $-CH_3$); ^{13}C NMR (62 MHz, $[D_6]DMSO$): $\delta = 165.2$ (C-4), 148.7 (C-2), 137.1 (C-6), 110.4 (C-5), 82.8 (C-4'), 80.2 (C-1'), 52.1 (C-3'), 40.8 (C-5'), 35.7 (C-2'), 12.0 ppm ($-CH_3$); IR (ATR): $\tilde{\nu}_{max} = 3491, 3221, 3114, 2828, 1696, 1599, 1569, 1472, 1368, 1284, 1267, 1157, 1108, 1045, 958, 760$ cm^{-1} ; MS (ESI): $m/z = 417.9$ $[M+H]^+$, 555.9 $[M+K]^+$; elemental analysis calcd (%) for $C_{10}H_{16}Cl_2N_4O_3Pd \cdot H_2O$: C 27.57, H 4.17, N 12.86; found: C 26.86, H 3.92, N 12.31.

cis-Dichloro(3',5'-diamino-3',5'-dideoxy-D-erythro-thymidine)-platinum(II) (5): With ligand **2** and $K_2[PtCl_4]$ (259.15 mg, 0.624 mmol); yield 297 mg (94%); 1H NMR (400 MHz, $[D_6]DMSO$): $\delta = 11.33$ (s, 1H; NH), 7.45 (s, 1H; H-6), 6.22–5.04 (m, 5H; H-1', NH₂), 3.62–3.40 (m, 2H; H-3, H-4), 2.78–2.14 (m, 4H; H-5', H-5'', H-2, H-2'), 1.80 ppm (s, 3H; $-CH_3$); ^{13}C NMR (100 MHz, $[D_6]DMSO$): $\delta = 163.71$ (C-4), 150.14 (C-2), 136.7 (C-6), 110.1 (C-5), 83.6 (C-4'), 80.1 (C-1'), 55.9 (C-3'), 44.9 (C-5'), 35.9 (C-2'), 11.9 ($-CH_3$); IR (ATR): $\tilde{\nu}_{max} = 3478, 3194, 3114, 2825, 1659, 1470, 1368, 1268, 1209, 1076, 1030, 952, 770, 697$ cm^{-1} ; MS (micro-ESI): $m/z = 529.1$ $[M+Na]^+$, 544.1 $[M+K]^+$; elemental analysis calcd (%) for $C_{10}H_{16}Cl_2N_4O_3Pt \cdot H_2O$: C 23.73, H 3.19, N 11.07; found: C 22.75, H 3.57, N 10.18.

cis-Dichloro(3',5'-diamino-3',5'-dideoxy-D-erythro-thymidine)-palladium(II) (6): With ligand **2** and $K_2[PdCl_4]$ (203.8 mg, 0.624 mmol); yield 246 mg (94%); 1H NMR (250 MHz, $[D_6]DMSO$): $\delta = 11.28$ (s, 1H; NH), 7.40 (s, 1H; H-6), 5.96 (dd, $J = 3.1, 5.3$ Hz, 1H; H-1'), 4.8 4.65, 4.55, 4.43 (m, 4H; NH₂), 3.41–3.18 (m, 4H; H-3', H-4', H-5', H-5''), 2.27–2.13 (m, 2H; H-2', H-2''), 1.78 ppm (s, 3H; $-CH_3$); ^{13}C NMR (60 MHz, MeOD): $\delta = 163.4$ (C-4), 149.9 (C-2), 136.2 (C-6), 109.9 (C-5), 82.97 (C-4'), 81.0 (C-1'), 54.2 (C-3'), 42.3 (C-5'), 36.1 (C-2'), 12.1 ppm ($-CH_3$); IR (ATR): $\tilde{\nu}_{max} = 3475, 3198, 3112, 2830, 1662, 1561, 1468, 1362, 1269, 1074, 1034, 953, 774, 705$ cm^{-1} ; elemental analysis calcd (%) for $C_{10}H_{16}Cl_2N_4O_3Pd \cdot H_2O$: C 27.57, H 4.17, N 12.86; found: C 27.12, H 4.23, N 12.22.

X-ray crystal structure of 4: The intensity data for the compounds were collected on a Nonius KappaCCD diffractometer by using graphite monochromated Mo-K α radiation. Data were corrected for Lorentz and polarization effects, but not for absorption effects.^[32,33] The structure was solved by direct methods (SHELXS^[34]) and refined by full-matrix least-squares techniques against F_o^2 (SHELXL-97).^[35] All hydrogen atoms were included at calculated positions with fixed thermal parameters. All nonhydrogen atoms were refined anisotropically.^[35] A XP (Siemens Analytical X-ray Instruments, Inc.) was used for structure representations. Crystal data for **4**:^[36] $C_{10}H_{16}Cl_2N_4O_3Pd \cdot H_2O$, $M_w = 434.56$ $g\ mol^{-1}$, yellow prism, size $0.05 \times 0.05 \times 0.05$ mm^3 , orthorhombic, space group $P2_12_12_1$, $a = 7.9191(7)$, $b = 9.7204(10)$, $c = 40.738(4)$ \AA , $V = 3135.9(5)$ \AA^3 , $T = -90^\circ C$, $Z = 8$, $\rho_{calcd} = 1.832$ $g\ cm^{-3}$, μ (MoK α) = 15.43 cm^{-1} , $F(000) = 1720$, 6491 reflections in $h(-9/6)$, $k(-11/11)$, $l(-51/52)$, measured in the range $2.15^\circ \leq \theta \leq 27.45^\circ$, completeness $\theta_{max} = 71.1\%$, 4101 independent reflections, $R_{int} = 0.0676$, 2903 reflections with $F_o > 4\sigma(F_o)$, 379 parameters, 0 restraints, $R1_{obs} = 0.0647$, $wR2_{obs} = 0.1313$, $R1_{all} = 0.1108$, $wR2_{all} = 0.1522$, GOOF = 1.053, Flack parameter $-0.03(8)$, largest difference peak and hole: $1.079/-1.222$ $e\ \text{\AA}^{-3}$.

Cell culture: The following human cell lines and their chemoresistant sublines were used: control vector and FADD-dn-transfected Burkitt-like lymphoma (BJAB) cells,^[37] which stably express a dominant negative FADD mutant lacking the N-terminal death effector domain (kindly do-

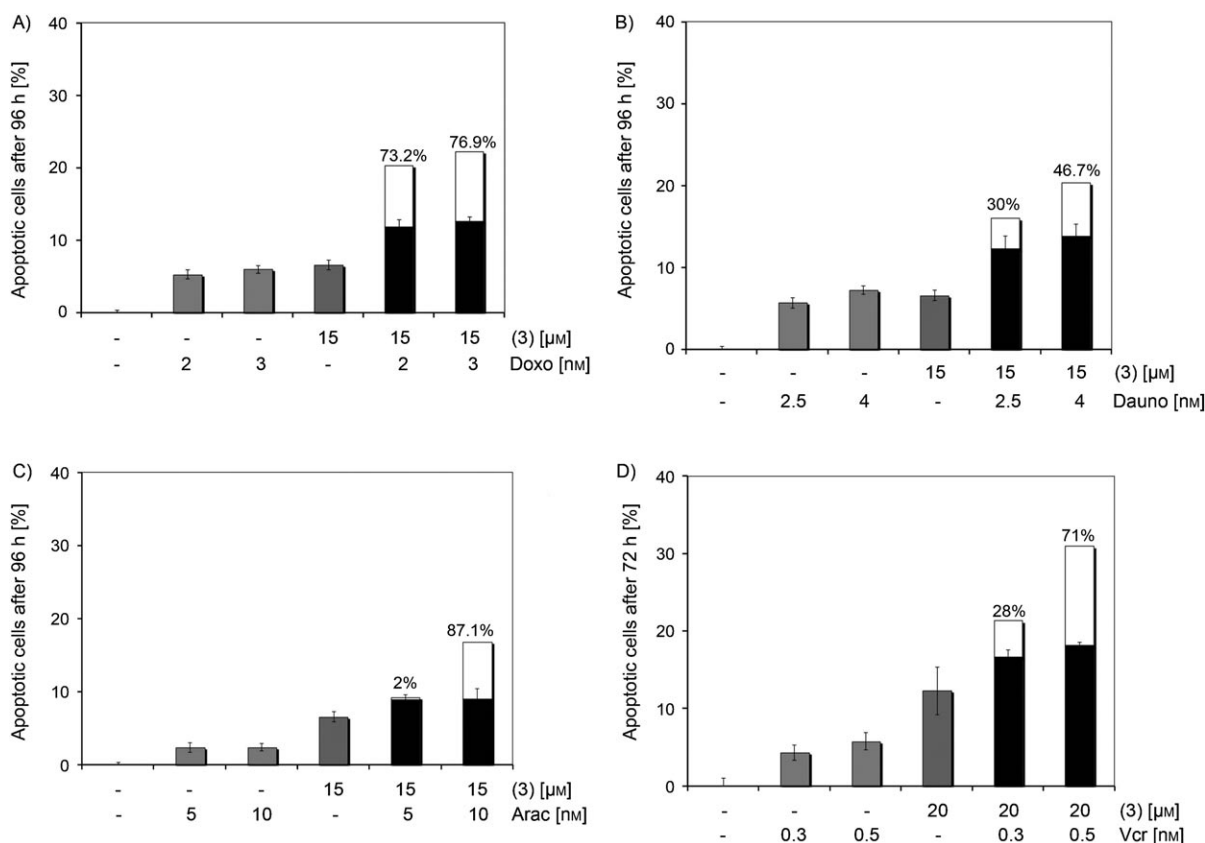


Figure 9. Synergistic effects. BJAB cells were treated with thymiplatin (15/20 μM) as well as with: A) doxorubicin (2/3 nM), B) daunorubicin (2.5/3 nM), C) cytarabine (5/10 nM), and D) vincristin (0.3/0.5 nM). DNA fragmentation was determined after 96 h (A, B, C) and 72 h (D). Combination of thymiplatin with these drugs resulted in an increase in DNA fragmentation. Values are given as percentages of cells with hypodiploid DNA ± S.D. (*n* = 3) (black areas = addition, white areas = synergy).

nated by Prof. Dr. S. Fulda, University of Ulm); control vector and Bcl-2 transfected melanoma cells (Mel-HO), which stably over-express the anti-apoptotic protein Bcl-2 (kindly provided by Dr. Eberle, Charité Berlin); the leukemia B-cell precursor (Nalm-6) and its vincristin and daunorubicin resistant sublines. All cell lines were cultured in RPMI 1640 supplemented with fetal calf serum (FCS; 10%), except for Mel-HO cells, which were cultured in DMEM with FCS (10%).

Measurement of cell death with the LDH release assay: Cytotoxicity was measured by using the release of lactate dehydrogenase (LDH) as described previously.^[38] After incubation with different concentrations of **3** for 2 h; LDH released by BJAB cells was measured in cell culture supernatants by using a cytotoxicity detection kit from Boehringer Mannheim (Mannheim, Germany). The supernatants were centrifuged at 300 g for 5 min. Cell-free supernatants (20 μL) were diluted with PBS (80 μL) and the reaction mixture (100 μL) was added. Then, the time-dependent formation of the reaction product was quantified photometrically at 490 nm. The maximum amount of LDH activity released by the cells was determined by lysis with Triton X-100 (0.1%) in culture medium and was set as 100% cell death.

Determination of cell concentration and cell viability: Cell viability was determined with the CASY[®] Cell Counter+Analyzer System from Schaefer System, GmbH (Reutlingen, Germany). Settings were specifically defined for the requirements of the cells used. With this system the cell concentration can be analyzed simultaneously in three different size ranges: cell debris, dead cells, and viable cells can be determined in one measurement.^[39] BJAB cells were seeded at a density of 1 × 10⁵ cells per mL and were treated with different concentrations of **3**; untreated cells served as control. After 24 h incubation the cells were resuspended, and 100 μL from each well was diluted in CASYton (10 mL; ready-to-use isotonic saline solution) for immediate automated count.

Measurement of DNA fragmentation: Apoptotic cell death was determined by using a modified cell-cycle analysis^[40] that detects DNA fragmentation at the single-cell level. For measurement of DNA fragmentation, cells were seeded at a density of 1 × 10⁵ cells per mL and treated with different concentrations of thymiplatin (**3**). After 72 h incubation, cells were collected by centrifugation at 300 g for 5 min, washed with PBS at 4°C and fixed in PBS/formaldehyde (2%, v/v) on ice for 30 min. After being fixed, the cells were incubated with ethanol/PBS (2:1, v/v) for 15 min, centrifuged, and resuspended in PBS containing RNase A (40 μg mL⁻¹). After incubation for 30 min at 37°C, the cells were centrifuged again and finally resuspended in PBS containing PI (50 μg mL⁻¹). Nuclear DNA fragmentation was then quantified by flow cytometric determination of hypodiploid DNA. Data were collected and analyzed by using a FACScan (Becton Dickinson, Heidelberg, Germany) equipped with the CELL Quest software. Data are given in % hypodiploidy (subG1), which reflects the number of apoptotic cells.

Measurement of the mitochondrial permeability transition: After incubation with different concentrations of **3**, BJAB cells were collected by centrifugation at 300 g at 4°C for 5 min. The mitochondrial permeability transition was then determined by staining the cells with 5,5,6,6-tetrachloro-1,1,3,3-tetraethyl-benzimidazolylcarbocyanin iodide (JC-1; Molecular Probes, Leiden, The Netherlands) as described.^[26,41] Cells (1 × 10⁵) were resuspended in phenol red-free RPMI 1640 (500 μL) without supplements, and JC-1 was added to give a final concentration of 2.5 μg mL⁻¹. The cells were incubated for 30 min at 37°C under moderate shaking. Control cells were likewise incubated in the absence of JC-1 dye. The cells were harvested by centrifugation at 300 g, 4°C for 5 min, washed with ice-cold PBS and resuspended in PBS (200 μL) at 4°C. The mitochondrial permeability transition was then quantified by flow cytometric determination of cells with decreased fluorescence, that is, those

with mitochondria displaying a lower membrane potential ($\Delta\Psi_m$). Data were collected and analyzed by using a FACScan (Becton Dickinson) equipped with the CELL Quest software. Data are given in % cells with low $\Delta\Psi_m$, which reflects the number of cells undergoing mitochondrial apoptosis.

Annexin V/propidium iodide binding assay: Early apoptotic rates were assessed with flow cytometry by using the annexin V-fluorescein isothiocyanate/PI kit (BD Pharmingen, San Diego, CA, USA), in which annexin V binds to exposed phosphatidylserine of early apoptotic cells,^[42,43] and PI stains cells that have an increased membrane permeability, that is, the late apoptotic cells. Samples were prepared according to the manufacturer's instructions. Flow cytometric analysis was performed by using a FACS-Calibur cytometer (Becton Dickinson, San Jose, CA, USA). The annexin V+/PI- cells were defined as early apoptotic cells.

Western blot analysis: After incubation for either 40 or 52 h with 3 (80 μM), BJAB cells were washed twice with PBS and lysed in buffer containing Tris-HCl (10 mM), pH 7.5, NaCl (300 mM), Triton X-100 (1%), MgCl_2 (2 mM), ethylenediamine tetra-acetic acid (EDTA; 5 μM), and one protease inhibitor cocktail tablet (Roche Diagnostics, Germany). Protein concentration was determined by using the bicinchoninic acid assay from Pierce (Rockford, IL, USA).^[44] Equal amounts of protein (usually 40 μg per lane) were separated by SDS-PAGE.^[45] Subsequently, blotting of protein onto nitrocellulose membrane (Schleicher and Schuell, Dassel, Germany) was performed exactly as previously described.^[46] After being blotted, the membrane was blocked for 1 h in PBST (PBS, 0.05% Tween-20) containing non-fat dry milk (5%) and incubated with primary antibody for 1 h. The membrane was then washed three times with PBST, and secondary antibody in PBST was applied for 1 h. Finally, the membrane was washed again in PBST and protein bands were visualized by using the ECL enhanced chemiluminescence system (Amersham Buchler, Braunschweig, Germany).

Acknowledgements

Financial support from the Japan–German exchange program was supported by JSPS and DFG. The European Commission (FP6, Marie Curie OIF), the Dr. Kleist-Stiftung Berlin (Germany), and the Dutch Polymer Institute (DPI, cluster HTE) are gratefully acknowledged.

- [1] B. Rosenberg, L. VanCamp, J. E. Trosko, V. H. Mansour, *Nature* **1969**, 222, 385–386.
- [2] L. Kelland, *Nat. Rev. Cancer* **2007**, 7, 573–584.
- [3] H. Choy, C. Park, M. Yao, *Clin. Cancer Res.* **2008**, 14, 1633–1638.
- [4] Z. H. Siddik, *Oncogene* **2003**, 22, 7265–7279.
- [5] R. Hrstka, D. J. Powell, V. Kvardova, E. Roubalova, K. Bourougaa, M. M. Candeias, P. Sova, F. Zak, R. Fahraeus, B. Vojtesek, *Anti-Cancer Drugs* **2008**, 19, 369–379.
- [6] P. C. A. Bruijninx, P. J. Sadler, *Curr. Opin. Chem. Biol.* **2008**, 12, 197–206.
- [7] K. J. Haxton, H. M. Burt, *J. Pharm. Sci.* **2009**, 98, 2299–2316.
- [8] S. H. van Rijt, P. J. Sadler, *Drug Discovery Today* **2009**, 14, 1089–1097.
- [9] M. Gottschaldt, U. S. Schubert, *Chem. Eur. J.* **2009**, 15, 1548–1557.
- [10] J. Möker, J. Thiem, *Eur. J. Org. Chem.* **2009**, 4842–4847.
- [11] C. G. Hartinger, A. A. Nazarov, S. M. Ashraf, P. J. Dyson, B. K. Keppler, *Curr. Med. Chem.* **2008**, 15, 2574–2591.
- [12] J. Zhang, X. J. Sun, K. M. Smith, F. Visser, P. Carpenter, G. Barron, Y. S. Peng, M. J. Robins, S. A. Baldwin, J. D. Young, C. E. Cass, *Biochemistry* **2006**, 45, 1087–1098.
- [13] J. C. Franke, M. Plotz, A. Prokop, C. C. Geilen, H. G. Schmalz, J. Eberle, *Biochem. Pharmacol.* **2010**, 79, 575–586.
- [14] D. Schlawe, A. Majdalani, J. Velcicky, E. Hessler, T. Wieder, A. Prokop, H. G. Schmalz, *Angew. Chem.* **2004**, 116, 1763–1766; *Angew. Chem. Int. Ed.* **2004**, 43, 1731–1734.
- [15] M. Maeda, N. Abiko, H. Uchida, T. Sasaki, *J. Med. Chem.* **1984**, 27, 444–449.
- [16] C. Nervi, M. A. Vigna, G. Cavigiolo, M. Ravera, D. Osella, *Inorg. Chim. Acta* **2005**, 358, 2799–2803.
- [17] T. S. Lin, R. X. Zhou, K. J. Scanlon, W. F. Brubaker, J. J. S. Lee, K. Woods, C. Humphreys, W. H. Prusoff, *J. Med. Chem.* **1986**, 29, 681–686.
- [18] D. Koth, M. Gottschaldt, H. Görls, K. Pohle, *Beilstein J. Org. Chem.* **2006**, 2.
- [19] A. Roth, D. Koth, M. Gottschaldt, W. Plass, *Cryst. Growth Des.* **2006**, 6, 2655–2657.
- [20] M. Gottschaldt, D. Koth, H. Görls, *Org. Biomol. Chem.* **2005**, 3, 1170–1171.
- [21] D. Koth, A. Fiedler, S. Scholz, M. Gottschaldt, *J. Carbohydr. Chem.* **2007**, 26, 267–278.
- [22] J. F. R. Kerr, A. H. Wyllie, A. R. Currie, *Br. J. Cancer* **1972**, 26, 239–257.
- [23] B. Fadeel, S. Orrenius, B. Zhivotovsky, *Biochem. Biophys. Res. Commun.* **1999**, 266, 699–717.
- [24] G. Majno, I. Joris, *Am. J. Pathol.* **1995**, 146, 3–15.
- [25] S. Van Cruchten, W. Van den Broeck, *Anat. Histol. Embryol.* **2002**, 31, 214–223.
- [26] I. H. Lambert, E. K. Hoffmann, F. Jorgensen, *J. Membr. Biol.* **1989**, 111, 113–132.
- [27] G. M. Cohen, *Biochem. J.* **1997**, 326, 1–16.
- [28] A. G. Porter, R. U. Janicke, *Cell Death Differ.* **1999**, 6, 99–104.
- [29] Q. A. Liu, M. O. Hengartner, *Ann. N.Y. Acad. Sci.* **2006**, 887, 92–104.
- [30] Y. A. Luqmani, *Princ. Pract. Med.* **2005**, 14, 35–48.
- [31] B. A. Chabner, D. L. Longo in *Cancer Chemotherapy and Biotherapy. Principles and Practice*, 4th ed., Lippincott Williams & Wilkins, Philadelphia, **2006**, pp. 12–18.
- [32] COLLECT, Nonius B.V., Netherlands, **1998**.
- [33] Z. Otwinowski, W. Minor in *Methods in Enzymology Vol. 276* (Eds.: C. W. Carter, R. M. Sweet), Academic Press, New York, **1997**, pp. 307–326.
- [34] G. M. Sheldrick, *Acta Crystallogr. Sect. A* **1990**, 46, 467–473.
- [35] G. M. Sheldrick, University of Göttingen (Germany), **1997**.
- [36] CCDC-650715 contains the supplementary crystallographic data for **4**. These data can be obtained free of charge from The Cambridge Crystallographic Data Centre via www.ccdc.cam.ac.uk/data_request/cif
- [37] T. Wieder, F. Essmann, A. Prokop, K. Schmelz, K. Schulze-Osthoff, R. Beyaert, B. Dorken, P. T. Daniel, *Blood* **2001**, 97, 1378–1387.
- [38] T. Wieder, C. E. Orfanos, C. C. Geilen, *J. Biol. Chem.* **1998**, 273, 11025–11031.
- [39] R. Voisard, P. C. Dartsch, U. Seitzer, D. Roth, M. Kochs, V. Hombach, *Vasa Suppl.* **1991**, 33, 140–141.
- [40] F. Essmann, T. Wieder, A. Otto, E. C. Muller, B. Dorken, P. T. Daniel, *Biochem. J.* **2000**, 346, 777–783.
- [41] M. Reers, S. T. Smiley, C. Mottola-Hartshorn, A. Chen, M. Lin, L. B. Chen, *Methods Enzymol.* **1995**, 260, 406–417.
- [42] V. A. Fadok, D. Xue, P. Henson, *Cell Death Differ.* **2001**, 8, 582–587.
- [43] R. A. Schlegel, P. Williamson, *Cell Death Differ.* **2001**, 8, 551–563.
- [44] P. K. Smith, R. I. Krohn, G. T. Hermanson, A. K. Mallia, F. H. Gartner, M. D. Provenzano, E. K. Fujimoto, N. M. Goeke, B. J. Olson, D. C. Klenk, *Anal. Biochem.* **1985**, 150, 76–85.
- [45] U. K. Laemmli, *Nature* **1970**, 227, 680–685.
- [46] T. Wieder, C. C. Geilen, M. Wieprecht, A. Becker, C. E. Orfanos, *FEBS Lett.* **1994**, 345, 207–210.

Received: March 29, 2010

Published online: October 27, 2010